

Document made available under the Patent Cooperation Treaty (PCT)

International application number: PCT/US05/005328

International filing date: 17 February 2005 (17.02.2005)

Document type: Certified copy of priority document

Document details: Country/Office: US
Number: 60/546,347
Filing date: 20 February 2004 (20.02.2004)

Date of receipt at the International Bureau: 07 April 2005 (07.04.2005)

Remark: Priority document submitted or transmitted to the International Bureau in compliance with Rule 17.1(a) or (b)



World Intellectual Property Organization (WIPO) - Geneva, Switzerland
Organisation Mondiale de la Propriété Intellectuelle (OMPI) - Genève, Suisse

1302407



THE UNITED STATES OF AMERICA

TO ALL TO WHOM THESE PRESENTS SHALL COME:

UNITED STATES DEPARTMENT OF COMMERCE

United States Patent and Trademark Office

March 31, 2005

THIS IS TO CERTIFY THAT ANNEXED HERETO IS A TRUE COPY FROM THE RECORDS OF THE UNITED STATES PATENT AND TRADEMARK OFFICE OF THOSE PAPERS OF THE BELOW IDENTIFIED PATENT APPLICATION THAT MET THE REQUIREMENTS TO BE GRANTED A FILING DATE.

APPLICATION NUMBER: 60/546,347

FILING DATE: February 20, 2004

RELATED PCT APPLICATION NUMBER: PCT/US05/05328



Certified by

Don W. Dudas

Under Secretary of Commerce
for Intellectual Property
and Director of the United States
Patent and Trademark Office

PROVISIONAL APPLICATION FOR PATENT COVER SHEET

This is a request for filing a PROVISIONAL APPLICATION FOR PATENT under 37 CFR 1.53(c).

Express Mail Label No. EL961005743US

1750 U.S. PTO
60/546347

022004

INVENTOR(S)			
Given Name (first and middle [if any])	Family Name or Surname	Residence (City and either State or Foreign Country)	
Jamey D. Minoru	MARTH FUKUDA	San Diego, California La Jolla, California	
Additional inventors are being named on the _____ separately numbered sheets attached hereto			
TITLE OF THE INVENTION (500 characters max)			
ANXIOLYTIC TREATMENT BY INHIBITION OF ST8SIA-II SIALYLTRANSFERASE			
Direct all correspondence to: CORRESPONDENCE ADDRESS			
<input checked="" type="checkbox"/> Customer Number:	25225		
OR			
<input type="checkbox"/> Firm or individual Name			
Address			
City	State	Zip	
Country	Telephone	Fax	
ENCLOSED APPLICATION PARTS (check all that apply)			
<input checked="" type="checkbox"/> Specification Number of Pages	30	<input type="checkbox"/> CD(s), Number	
<input checked="" type="checkbox"/> Drawing(s) Number of Sheets	7	<input checked="" type="checkbox"/> Other	Return postcard
<input checked="" type="checkbox"/> Application Data Sheet. See 37 CFR 1.76 (2 pages)			
METHOD OF PAYMENT OF FILING FEES FOR THIS PROVISIONAL APPLICATION FOR PATENT			
<input checked="" type="checkbox"/> Applicant claims small entity status. See 37 CFR 1.27.			FILING FEE AMOUNT (\$) 80.00
<input type="checkbox"/> A check or money order is enclosed to cover the filing fees.			
<input checked="" type="checkbox"/> The Director is hereby authorized to charge filing fees or credit any overpayment to Deposit Account Number: 03-1952			
<input type="checkbox"/> Payment by credit card. Form PTO-2038 is attached.			
The invention was made by an agency of the United States Government or under a contract with an agency of the United States Government.			
<input type="checkbox"/> No	<input checked="" type="checkbox"/> Yes, the name of the U.S. Government agency and the Government contract number are: National Institutes of Health - Grant Nos. DK48247, HL57345, and GM62116		

Respectfully submitted,

[Page 1 of 1]

Date February 20, 2004

 SIGNATURE Karen R. Zachow
 TYPED OR PRINTED NAME Karen R. Zachow, Ph.D.
 TELEPHONE (858) 720-5191

 REGISTRATION NO. 46,332
 (if appropriate)
 Docket Number: 220003065000
USE ONLY FOR FILING A PROVISIONAL APPLICATION FOR PATENT

I hereby certify that this correspondence is being deposited with the U.S. Postal Service as Express Mail, Airbill No. EL961005743US, in an envelope addressed to: MS Provisional Patent Application, Commissioner for Patents, P.O. Box 1450, Alexandria, VA 22313-1450, on the date shown below.

Dated: 2-20-04

Signature: [Signature] (Michael Boyd)

ANXIOLYTIC TREATMENT BY INHIBITION OF ST8SIA-II SIALYLTRANSFERASE

STATEMENT REGARDING FEDERALLY SPONSORED RESEARCH

[0001] This invention was made with government support under grant numbers DK48247, HL57345, GM62116 awarded by the National Institutes of Health. The government may have certain rights in this invention.

TECHNICAL FIELD

[0002] The present invention relates to the field of anxiety and fear disorders, particularly to treating such disorders through inhibition of sialyl transferase activity.

BACKGROUND OF THE INVENTION

[0003] The hippocampus and amygdala are involved in conditioned fear behavior. It is widely accepted that the amygdala is involved in fear memory (LeDoux, 2000; Maren, 2001). Fear associating with a single cue (a tone) paired with electrical shock requires the amygdala but not the hippocampus. However, fear associating the environment (the context) with shock requires both the amygdala and dorsal hippocampus (LeDoux, 2000; Anagnostaras et al., 2001; Maren, 2001). The passive avoidance task generally requires multiple neurotransmitter systems throughout the brain including the amygdala and hippocampus (Ammassari-Teule et al., 1991). There remains a need for effective therapies and agents for amelioration of anxiety and fear disorders.

[0004] All publications and patent applications cited herein are hereby incorporated by reference in their entirety.

BRIEF DESCRIPTION OF THE DRAWINGS

[0005] Fig. 1 depicts mutagenesis of the ST8Sia-II gene. Fig. 1a is a schematic showing wild-type *ST8Sia-II* allele for ST8Sia-II, plox targeting vector, mutant allele after homologous recombination in ES cells, and type I deleted () allele, represented with restriction enzyme sites. Polymorphism of *Bam*HI site is found and denoted by an asterisk. Black boxes are exons and triangles indicate loxP sequences. E, EcoRI; H, HindIII; X, XhoI. Fig. 1b depicts genotypes determined by Southern blot analysis of genomic DNA from ES cells and mouse tail tissue digested

by *Bam*HI. Fig. 1c (top panels) depicts total RNA isolated from the brains of wild-type (WT), heterozygous (WT/ Δ), and homozygous (Δ/Δ) mutant mice and used in RT-PCR with specific primer pairs for ST8Sia-II and ST8Sia-IV. RT-PCR analysis was also performed at 4 different ages (lower panels), postnatal day 0 (P0), 1 month old (1M), 3 months old (3M), and 6 months old (6M).

[0006] Fig. 2 depicts western blot analysis using anti-polysialic acid (PSA) antibody 5A5, and anti-NCAM antibody H28 of total protein extracts of different regions of the 8 week-old mouse brain from wild-type (wt/wt), heterozygous ST8Sia-II mutant (wt/ Δ), and homozygous ST8Sia-II mutant (Δ/Δ) littermates. A portion of the sample was digested with endo-N before the analysis. OB, olfactory bulb; HY, hypothalamus; HP, hippocampus; CX, cerebral cortex; CB, cerebellum.

[0007] Fig. 3 depicts polysialic acid staining of the hippocampus and subventricular zone of wild-type and ST8Sia-II deficient mice. Cryosections of hippocampus from wild-type (WT, a and b) and ST8Sia-II deficient (Δ/Δ , c and d) mice were stained with anti-PSA antibody, 12F8. Nissl staining is indicated in green and PSA in red. In WT mice, granule cells in the dentate gyrus are PSA-positive (arrowheads in b). In contrast to WT mice, note that precursor cells in the dentate gyrus are not labeled by 12F8 in Δ/Δ mice (d). PSA (red) was detected in subventricular zone from WT (e-g) and Δ/Δ (h-j) and nuclei (blue) were shown by Hoechst staining (e and h). Panels f, g, i, and j are magnifications of e and h as indicated. Migrating cells are PSA-positive in both genotypes (arrowheads in f and i). However, Δ/Δ has a few cells expressing PSA near anterior part of subventricular zone (arrowheads in j) compared to PSA-positive cells in WT (g). To label mitotic cells in embryonic and adult brains, BrdU was injected into a pregnant mouse at embryonic day 16 (k and n) and into adult mice at 2-3 months post-natal age (l, m, o, p), respectively. BrdU-labeled cells were visualized by anti-BrdU antibody (green) and nuclei were stained with Hoechst dye (blue). CC, corpus callosum; DG, dentate gyrus; G, granule cell layer; H, hilus; LV, lateral ventricle; S, striatum.

[0008] Fig. 4 depicts hippocampal mossy fiber topology. Timm's staining was performed (a-h) on brain tissue from denoted genotypes at various developmental stages, 2 weeks old (2W), 1 month old (1M), 3 months old (3M), and 6 months old (6M). From early in development, the infrapyramidal mossy fiber projection in ST8Sia-II -deficient mice is larger than in wild-type mice and extends into the CA3a region (arrows). Hippocampal sections from wild-type and ST8Sia-II

deficient mice (3 months old) were also stained with anti-calbindin (CaBP, i and j) and anti-NCAM (k and l) antibodies.

[0009] Fig. 5 depicts synapse formation in the stratum oriens of the hippocampal CA3 region. Fig. 5 a) PSA is expressed in suprapyramidal and infrapyramidal (arrowheads) mossy fibers of wild-type and ST8Sia-II deficient mice. The pyramidal cell layer also expresses polysialic acid (arrows). Fig. 5b) Synapse formation was compared by immunohistochemical staining with anti-synapsin I antibodies among wild-type (a-c) and ST8Sia-II deficient (d-f) mice. *b* and *e* are views of CA3c using higher magnification of boxed regions in *a* and *d*, respectively. Ectopic synapses (white arrows) are found in the ST8Sia-II -deficient mice. The CA3c region of wild-type (*c*) and ST8Sia-II mutant (*f*) mice also show difference in synapse formation.

[0010] Fig. 6 depicts short- and long-term potentiation in the hippocampal CA1 and CA3 regions. Fig. 6a) Theta-burst stimulation (TBS) of Schaffer collaterals (marked by arrow) evoked a strong increase in the slopes of fEPSPs recorded in the CA1 region of wild-type mice and in ST8Sia-II-deficient mice. Traces on the top show averaged fEPSPs recorded before and 50-60 minutes after induction of LTP in wild-type and ST8Sia-II deficient mice. Scale bars, 10 ms and 500 μ V. Fig. 6b) Single train of high-frequency stimulation of mossy fibers (1xHFS, marked by arrow) evoked a similar increase in amplitude of fEPSPs in the CA3 region of wild-type and ST8Sia-II deficient mice. Traces on the top show averaged fEPSPs recorded before and 50-60 min after induction of LTP. Scale bars, 10 ms and 50 μ V. In a-b, data shown are means + SEM. *n* indicates the number of slices and *N* indicates the number of mice.

[0011] Fig. 7 depicts metabolic and behavioral analyses. Fig. 7a) ST8Sia-II deficient mice displayed enhanced exploratory behavior in the open field test. The total distance traveled in a 30 min analysis was significantly increased in the ST8Sia-II deficient mice ($t_{(48)} = 2.65$, $p < .01$). The distance traveled in the center of the arena was also greater in the ST8Sia-II deficient mice ($t_{(48)} = 2.9$, $p < .005$). There was a trend for the ratio of the distance traveled in the center by the total distance traveled to be increased in the ST8Sia-II Δ/Δ mice ($p < .08$). Fig. 7b) In the passive avoidance test, the latency to enter the chamber was decreased in ST8Sia-II deficiency ($t_{(47)} = 2.79$, $p < .005$), suggesting impaired memory for the earlier noxious stimulus. ST8Sia-II deficient mice were also impaired in both the amygdale dependent cued version of the conditioned fear task ($t_{(48)} =$

2.56, $p < .01$ - the three tone only trials were collapsed for analysis) and the amygdala and hippocampal dependent contextual fear conditioning ($t_{(48)} = 2.23$, $p < .05$). Fig. 7c) Acoustic startle analysis indicated normal responses. Fig. 7d) In the water maze test, a repeated measures ANOVA analysis showed that both genotypes improved similarly across blocks of trials in the hidden platform (acquisition) trials and the t-test showed that the groups did not differ significantly in their probe trial performance. Fig. 7e) Automated analyses with metabolic cages and repeated ANOVA measures of the data revealed normal motor activity, food and water consumption, and caloric values (wt/wt, while circles; Δ/Δ black circles). There was no evidence of basal hyperactivity.

MODES OF CARRYING OUT THE INVENTION AND EXAMPLES

[0012] We have discovered that polysialic acid (PSA) formation by the ST8Sia-II polysialyltransferase, and in collaboration with NCAM, is an important determinant in the formation of neural circuits operating in the acquisition of fear behavior. We have observed that deficiency in expression of the ST8Sia-II polysialyltransferase alters fear responses normally processed by both the hippocampus and amygdala. The hippocampus and amygdala are involved in conditioned fear behavior. We have observed that the unique spectrum of effects in ST8Sia-II deficiency was associated with an increase in exploratory behavior and reduced responses to fear conditioning. Thus, we have discovered methods and agents for treating anxiety, fear, depression and other disorders of the CNS that pertain to anxiety and fear behavior.

[0013] The present invention provides methods for ameliorating a symptom of anxiety and fear behavior in a subject in need thereof by decreasing ST8Sia-II polysialyltransferase activity in the subject. This decrease in activity may be attained in a number of ways including, but not limited to, through a decrease in ST8Sia-II polysialyltransferase gene transcription and/or translation, a decrease in ST8Sia-II polysialyltransferase RNA stability and/or half-life, a decrease in ST8Sia-II polysialyltransferase stability and/or half-life, and through administration of a ST8Sia-II polysialyltransferase antagonist. Agents that decrease expression of the ST8Sia-II polysialyltransferase are thus of use in the methods of the invention. In another aspect, the invention provides screening methods for identifying agents for use in reducing anxiety through use of the ST8Sia-II polysialyltransferase gene. This includes the use of human ST8Sia-II polysialyltransferase gene as well as other animal homologues. The invention also provides non-

human transgenic mammals and inbred strains, including mice, for the study of anxiety and fear behavior.

[0014] The examples provided herein are to illustrate, but not limit, the invention.

Mutagenesis of the mouse *ST8Sia-II* gene

[0015] A region of the murine *ST8Sia-II* allele was isolated from a mouse129/SvJ genomic DNA library and used to construct a targeting vector. An *EcoRI-XhoI* fragment containing exon was flanked by two loxP sequences as described (Marth, 1996). Targeted ES clones were identified by polymerase chain reaction, and characterized by genomic Southern blotting. Multiple ES clones bearing the systemic (type I) deletion of the targeted *ST8Sia-II* allele were obtained after transient expression of Cre recombinase. Targeted ES cells were injected into C57BL/6 blastocysts to generate chimeric mice. Mutant *ST8Sia-II* alleles were maintained on the C57BL/6 background for more than 6 generations prior to mouse phenotype analysis.

RNA analyses

[0016] Total RNA was purified from brains at different ages by using Trizol solution (Invitrogen) and used for Northern hybridization and RT-PCR as described previously (Ong et al., 1998). RT-PCR was performed using cDNAs synthesized with oligo(dT) as a primer by Superscript II reverse transcriptase (Invitrogen) and 10 pmol of primers set for murine *ST8Sia-II* (mX) or *ST8Sia-IV* (mP). The following primers were used: mX-Tg1: 5'-CTGGAGGCAGAGGTACAATCAGATC-3' (nucleotides 104-128) and mX-Tg2: 5'-CCTCAAAGGCCCGCTGGATGACAGA-3' (nucleotides 646-622); mP-Tg1: 5'-AGGCTGGCTCCACCATCTTCCAACA-3' (nucleotides 173-197) and mP-Tg2: 5'-CTCTGTCACTCTCATTCGAAAGCC-3' (nucleotides 625-601).

Western blot analysis

[0017] After brains were removed, various brain regions were dissected and homogenized with RIPA buffer (150 mM NaCl; 50 mM Tris-HCl, pH 7.4; 1% NP40; 0.1% SDS; 5 mM EDTA) containing proteinase inhibitor cocktail (Roche Applied Science). Equivalent amounts of proteins were loaded onto a 5% SDS-PAGE gel, and transferred onto PVDF membranes (Millipore). Some

tissue extracts were incubated with endo-N (Hallenbeck et al., 1987) for 1 hour at 37°C prior to loading. Membranes were blocked with 10% dry milk in 20 mM Trisbuffered saline, pH 7.6, containing 0.1% Tween-20 (TBST), incubated with either mouse anti-PSA 5A5 (Developmental Studies Hybridoma Bank, diluted 1:1000 in TBST) or rat anti-NCAM H28 (Immunotech, diluted 1:200), and followed by peroxidase-conjugated antimouse IgM (1:4000) or anti-rat IgG (1:3000), respectively to detect by ECL kit (Amersham Biosciences).

5-Bromo-2'-deoxyuridine (BrdU)-labeling

[0018] BrdU (20 mg/ml in 0.007N NaOH and 0.9% NaCl) was injected (intraperitoneal) into the ST8Sia-II -deficient and wild-type mice (50 mg/kg body weight) for 5 times at 2 hour intervals over an 8 hour period. One week after the last administration, the mice were deeply anesthetized with Avertin (0.015 ml/g body weight) and brains were removed. The brains were fixed with Carnoy (60% ethanol, 30% chloroform, 10% acetic acid) and embedded in paraffin to cut sagittal or coronal sections at 10 μ m. Every third section was collected and 10 sections, which cover 300 μ m in the center of the hippocampus, were stained for BrdU. BrdU-positive cells were detected by BrdU specific monoclonal antibody (Roche Applied Science) and Alexa Fluor® 488 goat anti-mouse IgG1 (Molecular Probes). To measure distribution of embryonic neural stem cells in brains, BrdU was administrated into pregnant heterozygous mice (100 mg/kg at embryonic day 16, E16) that were mated with heterozygous male mice. Brains from neonatal mice and 10 days postnatal mice were fixed and stained as described above.

Histology

[0019] To stain sections with SMI-32 (Sternberger Monoclonal), Tuj1 (BAbCo), and antibodies for synapsin I (Chemicon), GFAP or MAP2 (Roche Applied Science), sections were prepared as described for BrdU detection. To stain sections with anti-PSA 12F8 (BD Biosciences), anti-NCAM H28, and anti-calbindine D-28K (Chemicon), mice were perfused intracardially with phosphate-buffered saline (PBS) followed by 4% paraformaldehyde in 0.1 M phosphate buffer, pH 7.4. Sagittal or coronal sections frozen in OCT compound (Sakura Finetek) were cut at 30 μ m by a cryostat and collected onto PBS. The sections were treated with 0.3% H₂O₂ for 5 min, and incubated with PBS containing 0.1% normal goat serum and 0.25% Triton-X 100. Sections were

then treated with primary antibodies in the above blocking solution, followed by appropriate biotinylated secondary antibodies (Zymed and Vector Laboratories). The sections were treated with ABC reagent and DAB substrate (Vector Laboratories), transferred onto slides, and counterstained with cresyl violet. For immunofluorescence staining, tissues were incubated with primary antibodies in 1% normal goat serum and followed by Alexa Fluor® 488 or 594 conjugated goat anti-rabbit IgG, -rat IgM, -mouse IgG1, and -mouse IgG2a (Molecular Probe). Then the sections were reacted with Hoechst 33342 (Sigma) in PBS before mounting. With some slides, Nissl staining was performed with NeuroTracer™ Fluorescent Nissl Stains (Molecular Probe).

[0020] For Timm's staining, mice were perfused intracardially first with 15-50 ml of 0.37% sodium sulfide solution, followed by 4% paraformaldehyde in PBS to prepare frozen sections as described above. The sections were incubated in darkness for 40 min in a solution containing 30% gum arabic, 2.55% citric acid, 2.35% sodium citrate, 1.7% hydroquinone, and 0.1% silver nitrate. The slides were then rinsed in running water for 10 minutes and counterstained with cresyl violet.

Electrophysiology

[0021] Hippocampal slices from five- to six-month-old ST8Sia-II -deficient mice and their wild-type littermates were used for recordings. After halothane anesthesia, decapitation and removal of the brain, the hippocampi were cut with a VT 1000M vibratome (Leica, Nussloch, Germany) in slices 300 µm thick in ice-cold artificial cerebrospinal fluid (ACSF) containing (in mM): 250 sucrose, 25 NaHCO₃, 25 glucose, 2.5 KCl, 1.25 NaH₂PO₄, 2 CaCl₂, and 1.5 MgCl₂, pH 7.3. The slices were then kept at room temperature in a chamber filled with carbogenbubbled ACSF, containing 125 mM NaCl instead of 250 mM sucrose, for at least 2 hr before the start of recordings (modified from Edwards et al., 1990). In the recording chamber, slices were continuously superfused with carbogen-bubbled ACSF (2-3 ml/min) at room temperature.

[0022] For recordings in the CA3 region the slices were prepared as for recordings in the CA1 region, but with some modifications. Before decapitation, mice were transcardially perfused with ice-cold ACSF, containing (in mM): 250 sucrose, 25 NaHCO₃, 25 glucose, 2.5 KCl, 1.25 NaH₂PO₄, 0.5 CaCl₂, and 6 MgCl₂, pH 7.3. Slices were cut according to Claiborne and colleagues (1993). Exchange of sucrose-containing ACSF with normal (containing 2.5 mM CaCl₂ and 1.5 mM MgCl₂) was performed gradually using peristaltic pumps.

[0023] Schaffer collateral-CA1 extracellular recordings of focal fEPSPs were obtained from the *stratum radiatum* of the CA1 region in response to stimulation of Schaffer collaterals by an electrode placed approximately 400 μ m apart from the recording electrode in the *stratum radiatum* of the CA1 region. Recordings and stimulations were performed with glass pipettes filled with ACSF having a resistance of 2 M Ω . Basal synaptic transmission was monitored at 0.033 Hz. The slices were maintained at room temperature. Homosynaptic LTP in the CA1 region was induced by theta-burst stimulation (TBS) applied orthodromically to Schaffer collaterals and recorded extracellularly in the *stratum radiatum*. A TBS consisted of 10 bursts delivered at 5Hz. Each burst consisted of 4 pulses delivered at 100 Hz. Duration of pulses was 0.2 ms, and five TBSs were applied every 20 s to induce LTP (Eckhardt et al., 2000). The stimulation strength was in the range of 40-70 μ A to provide fEPSPs with an amplitude of 50% of the subthreshold maximum. The mean slope of fEPSPs recorded 0-10 min before TBS was taken as 100 %. The transient potentiation immediately following TBS (or STP, short-term potentiation) was measured as a maximal increase in the fEPSP slope during 1 min after LTP induction. The values of LTP were calculated as increase in the mean slopes of fEPSPs measured 50-60 min after TBS.

[0024] Mossy fiber-CA3 extracellular recordings and stimulations were both performed with glass pipettes filled with ACSF and having a resistance of 2 M Ω with stimulation strength of approximately 40 μ A. The stimulating electrode was placed close to the internal side of the granule cell layer. The recording pipette was placed in the *stratum lucidum* of the CA3 region. The mossy fiber responses selected for recording were of 40-60 μ V, with a fast rise-time and decay of fEPSPs (total duration of fEPSP < 10 ms, rise time < 3.5 ms), large paired pulse facilitation (> 170%), and prominent frequency facilitation (> 200%). The selected responses had no hallmarks of polysynaptic activation, such as jagged decay phase with multiple peaks, or variable latencies of fEPSPs.

[0025] The LTP-inducing high-frequency stimulation (HFS) consisted of one train of stimuli applied at 100 Hz during 1 sec once ("weak" stimulation protocol) or repeated four times with an interval of 20 sec ("strong" stimulation protocol). To evoke LTP exclusively in mossy fiber synapses, which are known to undergo LTP in a NMDA receptor-independent manner, the NMDA receptor antagonist AP-5 (50 μ M; Tocris, Bristol, UK) was applied 15 minutes before and during

HFS. All recorded mossy fiber responses followed presynaptic stimulation of 100 Hz and showed no changes in the shape of responses after induction of LTP. To additionally confirm that the fEPSPs recorded were evoked by the stimulation of mossy fibers and not by the associational/commissural pathway, an agonist of type II metabotropic glutamate receptors (L-CCG1, 10 μ M; Tocris), which is known to reduce synaptic transmission in CA3 mossy fiber synapses, was applied at the end of each experiment. Slices in which responses were reduced by at least 70% were selected for analysis. Basal synaptic transmission was monitored at 0.033 Hz. The mean amplitude of fEPSPs recorded 0-10 min before HFS was taken as 100%. Post-tetanic potentiation (PTP) was calculated as the maximal increase in the amplitude of fEPSP after HFS. The values of LTP were calculated as increase in the mean amplitude of fEPSPs measured 50-60 min after HFS.

[0026] Data acquisition and measurements were performed using an EPC-9 amplifier and Pulse software (Heka Elektronik, Lambrecht/Pfalz, Germany). Values in electrophysiological experiments are reported as mean \pm SEM (standard error of the mean). Student's *t*-test was used to assess statistical significance using Sigma Plot 5.0 software (SPSS, Chicago, IL, USA).

Nerve tract tracing between hippocampus and amygdala

[0027] Neuronal tracing between hippocampus and amygdala was analyzed in eight mice of each genotype by injecting biotinylated dextran amine (BDA, Molecular Probes) into the amygdala. After the mouse was deeply anesthetized with ketamine (1.25 mg/g) and xylazine (0.07 mg/g), BDA (10% in 0.1 M phosphate buffer, pH 7.4; 0.2 μ L) was stereotactically injected into amygdala by using Picospritzer (Parker Instrumentation) and the coordinates (A: -0.12, L: -0.27, D: -0.4 in cm from Bregma; Franklin and Paxinos, 1996). The animals were allowed to recover under close observation and returned to their cage. Six days after injection, brains were fixed as described above and cryosections were analyzed immunohistochemically using FITC-labeled Avidin (Vector Laboratories).

Metabolic and behavioral parameters

[0028] Two separate cohorts of four month-old male mice were analyzed. The first cohort of mice consisted of 9 ST8Sia-II deficient (Δ/Δ) mice and 10 wild -type (wt/wt) littermate controls.

These were assessed in a behavioral test battery modified from that used by McIlwain et al. (2001) and described in detail previously (Corbo et al., 2002), and included parameters such as metabolic performance, physical appearance, sensorimotor reflexes, motor activity, nociception, acoustic startle, sensorimotor gating, and assessments of learning and memory. Concern that testing mice in such a large battery could influence the behavior in any individual task, and that multiple assessments increases the probability of a Type I statistical error, a second cohort of mice (wt/wt: n=16; Δ/Δ : n=15) was analyzed in fear conditioning tasks and the open field test. In addition, a subset of this second cohort (wt/wt: n=12; Δ/Δ : n=9) was subsequently analyzed in the water maze (a task not run with the first cohort) and some of these mice (wt/wt n=8; Δ/Δ n=8) were also assessed for metabolic measures.

[0029] In the open field test, exploratory locomotor activity was measured in a 30 minutes test period in an area of 45 X 45 cm using a Digiscan apparatus (Accuscan Electronics, Columbus, OH). Vertical activity (rearing) total distance (cm), and center distance were recorded. The center distance divided by the total distance traveled is an indicator of anxiety-related behavior.

[0030] The water maze task constituted a pre-training phase during which all mice were tested for two days in a straight-swim pre-training protocol. Mice received 16 trials (8 trials over two days) in a 31 x 60 cm rectangular tank that was located in a different room than the circular tank used in the hidden platform trials. The platform was located 1 cm below the water opposite from the start location. Latency to climb onto the platform was the dependent measure. Criteria for advancing to the hidden platform trials was completing 6 of 8 trials under 10 seconds on the second day. This pretraining procedure provided experience with swimming and climbing onto a submerged platform without exposing the mice to the spatial cues used in the hidden platform trials. This procedure both screens for mice with severe motor deficits and reduces behavioral variability often seen on the first day hidden platform testing. All mice successfully passed this pretraining phase. Hidden platform testing followed in which extra-maze visual cues were hung from a curtain located around a 1.26-meter diameter circular tank. The water was made opaque with the addition of non-toxic paint. The 10 cm diameter escape platform was located 1 cm below the surface of the water and a Polytrack video-tracking system (San Diego Instruments) was used to collect mouse movement data (location, distance and latency) during training and probe trials. Each mouse was

given 8 trials a day, in 2 blocks of 4 trials for four consecutive days. After 36 trials, each animal was given a 60 sec probe trial. During the probe test, the platform was removed and quadrant search times were measured. Visual cue testing was performed 1 day after the last hidden-platform training trial, wherein mice were trained to locate a visible-cued platform. The visible cue was a gray plastic cube (9 cm) attached to a pole such that it was 10 cm above the platform. On each trial of the visible platform test, the platform was randomly located in one of the four quadrants. Mice were given 8 trials, in blocks of four trials, and the latency to find the platform was recorded for each trial.

[0031] Fear conditioning tests involved chambers (26 X 22 X 18 cm high) made of clear Plexiglas were placed in a 2 X 2 array (Med Associates). A video camera was connected to a video-based system for digital recording and subsequent analysis of freezing behavior upon mild electric shock (FreezeFrame, Actimetrics, St. Evanston, IL). The conditioned stimulus (CS) was an 85db 2,800 Hz 20-second tone and the unconditioned stimulus (US) was a scrambled foot shock at 0.75 mA presented during the last 3 seconds of the CS. Mice were placed in the test chamber for 3 minutes before the CS and freezing behavior was recorded. Freezing was defined as the absence of movement other than breathing and thresholds were selected via the software of high correlation with human observers. Three CS/US pairings are given with 1 minute spacing and freezing during the CS was also recorded. Twenty-four hours later each mouse was placed back into the shock chamber and freezing response was recorded for 3 minutes (context test). Two hours later, the chambers were modified to present a different environmental context (e.g. shape, odor, color changes) and the mouse was placed in this novel environment. Freezing behavior was recorded for 3 minutes before and during three CS presentations (cued conditioning). The time spent freezing was converted to a percent value.

[0032] For the passive avoidance analysis, a two-compartment light/dark apparatus (35 x 18 x 30 cm, Coulbourn Instruments, Allentown, PA) was used. Each mouse was placed individually in the lighted compartment. When the animal entered the dark compartment, a guillotine door closed behind the mouse and a foot shock of 0.4 mA was delivered through the grid floor of the dark compartment for 3 seconds. If the mouse did not enter the dark compartment within 10 minutes, it

was excluded from the retrieval test. In the retrieval trial performed 24 hours later, the latency for the mice to enter the dark compartment was recorded. The maximum latency was 600 seconds.

[0033] Metabolic chambers termed CLAMS (Comprehensive Lab Animal Monitoring System; Columbus Instruments, Columbus, OH) automatically recorded metabolic parameters including volume of carbon dioxide produced (VCO_2), volume of oxygen consumed (VO_2), respiration ($RER = VCO_2/VO_2$), and caloric (heat) value ($(3.815 + 1.232 \times RER) \times VO_2$), motion in all three axes in time, and consumption of food and water. Data was collected every 30 minutes over three 12 hour dark cycles and two 12 hour light cycles and analyzed as mean values over each 12 hour period with the exception of food and water intake which were added to the total during subsequent cycles.

[0034] Pulmonary function was scored by measurement of the uptake of carbon monoxide (CO). A carbon monoxide uptake monitor (Columbus Instruments, Columbus, OH) measured the CO level in a sealed chamber after exposing the mouse to a 60 second interval of air with 0.17 % CO. The mean breath per minute was also recorded. Each animal was tested once.

[0035] Blood pressure was determined by a non-invasive blood pressure tail-cuff system (Columbus Instruments) that measures systolic blood pressure in addition to heart rate and relative changes in diastolic and mean blood pressure. Individual mice were placed in a small cylinder chamber, occlusion and sensor cuffs were placed on the tail, and the tail was warmed to 37 C. Mice were first acclimated to the restraining chamber, tail cuffs, and the heat fan for 30 minutes for two days prior to testing. The mean of 4 measurements on the third day is reported and analyzed by the Student t-test.

ST8Sia-II deficiency in the mouse germline

[0036] The *ST8Sia-II* gene is highly conserved among mammals and includes multiple exons that divide the catalytic domain (Yoshida et al., 1996). Exon 4 encodes a significant portion of the sialylmotif L, a peptide region that takes part in donor substrate recognition and is essential for sialyltransferase activity (Datta and Paulson, 1995). DNA encoding exon 4 of the *ST8Sia-II* gene was targeted for elimination from the mouse genome (Fig. 1a). Targeted ES cells were transfected with Cre recombinase to delete loxP-flanked exon 4 sequence, and ES clones that bore the type I deletion were selected for Southern hybridization (Fig. 1b). Type I ES cells were identified and

injected into C57BL/6 blastocysts to obtain chimeric mice. Subsequently the mutant allele was transmitted into germline and bred into the C57BL/6 strain. Mice homozygous for the type I (deleted,) *ST8Sia-II* allele appeared to have no significant abnormality in body weight or brain size up to 6 months of age, in spite of the fact that high level expression of ST8Sia-II occurs in wild-type embryos at early developmental stages. Breeding from heterozygous males and females produced mice with genotypes close to Mendelian ratios (wt/wt : wt/ Δ : Δ / Δ = 29: 50: 21%; n=255), implying that the mutated ST8Sia-II allele was not deleterious in mouse development.

[0037] To confirm disruption of ST8Sia-II at mRNA level, Northern hybridization and RTPCR were performed. These analyses revealed that the truncated form of ST8Sia-II mRNA lacking exon 4 and an intact sialyl motif is present in both heterozygous and the ST8Sia-II null mice (Fig. 1c). The sequence of the mutant ST8Sia-II mRNA indicated that a truncated form of ST8Sia-II protein lacking exon 4 might be translated by in-frame splicing of exon 3 to exon 5. However, the truncated ST8Sia-II protein was shown to lack polysialyltransferase activity by immunofluorescence staining with PSA antibodies of the cells transfected with the mutant ST8Sia-II cDNA (data not shown). Northern hybridization and RT-PCR also demonstrated that the disruption of ST8Sia-II does not affect the level of ST8Sia-IV mRNA in ST8Sia-II deficient mice (Fig. 1c).

Regional defects in brain polysialic acid expression

[0038] Histological examination of macroscopic brain structure indicated normal development in the absence of ST8Sia-II activity (data not shown). Although NCAM-deficient mice have a smaller olfactory bulb and thicker rostral migratory stream (RMS) (Tomasiewicz et al., 1993; Cremer et al., 1994; Hu et al., 1996), ST8Sia-II deficient mice bear a normal size olfactory bulb and RMS (data not shown), as was also observed in ST8Sia-IV deficient mice (Eckhardt et al., 2000).

[0039] PSA expression in ST8Sia-II deficient mice was altered in comparison with wild-type littermates, being reduced though not eliminated in the olfactory bulb and cerebral cortex of 8-week-old adult mice (Fig. 2). There was no apparent quantitative alteration of PSA levels in the hypothalamus, hippocampus, and cerebellar cortex. A closer examination of the hippocampus revealed an altered pattern of PSA expression among ST8Sia-II deficient mice (Fig. 3a, d). The hippocampus is one of the regions that produce PSA in adults, and PSA is normally highly

expressed in granule cells, hilus, and mossy fibers. Neurogenesis in the dentate gyrus takes place throughout adulthood and neuronal progenitor cells are located at the border between the hilus and the granule cell layer. Newly generated cells migrate into the granule cell layer and normally express high levels of PSA. In the four groups of wildtype mice examined at different ages, progenitor cells bearing PSA decreased with increased age as expected (Kuhn et al., 1996). Among ST8Sia-II deficient littermates, the number of granule cells expressing PSA was markedly reduced and in some cases none were detected (Fig. 3b, d).

[0040] The subventricular zone (SVZ) is another area of neural stem cell genesis in the adult brain. Among wild-type mice, PSA is easily detectable in the anterior region of the SVZ (SVZa), likely indicating migrating neuroblasts, and is positive in the region of the striatum. Among ST8Sia-II deficient mice, PSA is also detectable in the SVZa and the striatum (Fig. 3e, f, h, i). Levels of PSA in the migratory pathway and the chain migration pattern of precursor cells appeared to be unchanged (Fig. 3f, i), consistent with results of staining by GFAP and β -tubulin antibodies (data not shown). However, in contrast to wild-type littermates, PSA was greatly reduced among newly generated neural cells along the lateral ventricle (Fig. 3g, j). These results indicate that PSA on neural precursor cells in the SVZ is synthesized primarily by the ST8Sia-II polysialyltransferase.

[0041] Deficiency of PSA formation in the context of neurogenesis was further examined by BrdU-labeling of neural precursors. At embryonic day 16, these cells are distributed in the hippocampus as well as the cortex. The labeled cell number and migration pattern in the dentate gyrus and the pyramidal cell layer were not distinguishable between wild-type and ST8Sia-II deficient mice (Fig. 3k, n). Even in adult, BrdU-positive mitotic cells were found in dentate gyrus and SVZ of both genotypes (Fig. 3l, m, o, p). The number of BrdU-positive cells in the adult dentate gyrus of ST8Sia-II deficient mice was not significantly lower than that of wild-type mice (wt/wt: 10.9 ± 2.9 , $n=4$; Δ/Δ : 8.7 ± 2.0 , $n=4$; $P>0.05$). These findings support the view that PSA formation in neural progenitor cells is provided primarily by ST8Sia-II, and show that PSA deficiency due to ST8Sia-II depletion does not affect the frequency of cells undergoing DNA replication in neurogenesis.

Altered axonal targeting and ectopic synapse formation

[0042] Hippocampal mossy fibers arise from granule cells in the dentate gyrus and target to the hippocampal CA3 region, fasciculating to become a thick suprapyramidal fiber projection. In addition, sprouting fibers from the dentate gyrus normally form a much thinner infrapyramidal mossy fiber projection along the border between the pyramidal cell layer and stratum oriens. This infrapyramidal projection is usually shorter than the suprapyramidal mossy fiber projection and terminates or merges with the suprapyramidal projection around CA3c. However, in the ST8Sia-II deficient mice, the suprapyramidal mossy fiber projection tended to be thinner and the infrapyramidal projection was thicker. Moreover, the infrapyramidal mossy fibers often extended to the far CA3a region (Fig. 4). This aberration was already present at the age of 2 weeks, and was prominent in all older ages examined. The same pattern was found by immunostaining of NCAM protein and calbindin expression (Fig. 4). Timm's staining further revealed many fine mossy fibers invading pyramidal cell layers in the CA3 region in ST8Sia-II deficient mice, forming a web-like structure between these two mossy fiber projections (CA3b and c). Visualization of cellular features by cresyl violet staining showed that the number and the pattern of granule and pyramidal cells were not different between wild-type and mutant animals (data not shown). Thus the aberrant pattern of mossy fiber projections caused by the absence of ST8Sia-II was not due to disarrangement of pyramidal cells in the CA3 region.

[0043] Mossy fiber axons are normally polysialylated and express NCAM, while pyramidal cells appear to express low levels of PSA. ST8Sia-IV deficient mice were previously found to lack PSA on mossy fibers but expressed PSA on neural precursors in the dentate gyrus at the age of 6 weeks (Eckhardt et al., 2000). In ST8Sia-II deficient mice, both suprapyramidal and infrapyramidal mossy fibers express PSA like their wild-type littermates (Fig. 5a). Suprapyramidal mossy fibers normally form synapses in the stratum oriens of CA3a. In contrast, the infrapyramidal mossy fibers normally synapse at CA3c and typically do not form synapses in the stratum oriens of CA3a. In the ST8Sia-II deficient mice, the infrapyramidal mossy fibers target into the stratum oriens of CA3a area and form ectopic synapses (Fig. 5b). In addition, mossy fibers extending along the ventral side of granule cell layer are often observed in the ST8Sia-II deficient mice and these also form ectopic

synapses. These findings demonstrate alterations in neuronal circuitry in the hippocampus due to the absence of ST8Sia-II.

Hippocampal synaptic plasticity

[0044] The most widely studied form of plasticity, LTP in the CA1 region of the hippocampus, has been reported to be abnormal in NCAM and ST8Sia-IV deficient mice (Muller et al., 1996; Eckhardt et al., 2000). Moreover, removal of PSA from hippocampal cultures of wild-type mice by endo-N prevented both LTP and LTD (Becker et al., 1996; Muller et al., 1996). In our studies, theta-burst stimulation (TBS) of Schaffer collaterals reliably produced short-term potentiation (STP) and LTP in all slices measured from wild-type animals (Fig. 6a). The mean level of STP measured as maximal potentiation during 1 min after TBS was $216.0 \pm 10.7\%$ and the level of LTP seen 50–60 min after TBS was $129.3 \pm 4.3\%$ (number of slices $n=8$, number of mice $N=3$). The levels of STP and LTP in ST8Sia-II deficient mice ($218.2 \pm 7.6\%$ and $127.9 \pm 5.3\%$, respectively; $n=8$, $N=3$) were not significantly different from wild-type mice. Stimulus-response curves for fEPSPs evoked by stimulation of Schaffer collaterals and the mean amplitudes of responses being 50% of the supramaximal levels were not different between ST8Sia-II deficient mice and wild-type littermates, thus demonstrating normal basal levels of excitatory transmission (data not shown).

[0045] LTP at mossy fiber synapses with CA3 pyramidal cell has been reported to be abnormal in NCAM deficient mice (Cremer et al., 1998). These synapses are important for hippocampal learning and memory formation (Lisman, 1999; Henze et al., 2000). CA3 LTP has features clearly distinct from CA1 LTP, being independent of postsynaptic NMDA receptors, but mediated by an elevation in cyclic adenosine monophosphate (cAMP) and activation of adenylate cyclase and PKA (Weisskopf et al., 1994). Field EPSPs evoked in CA3 pyramidal cells by mossy fiber stimulation were identified using a number of criteria (see Materials and methods) and showed properties typical for mossy fiber responses: Lowfrequency stimulation (0.33 Hz) potentiated fEPSPs to approximately 250% in wild-type and ST8Sia-II deficient mice. Application of L-CCG1 reduced the amplitude of fEPSPs similarly in both genotypes by 80%. The NMDA receptor antagonist AP-5 did not affect the amplitude of recorded fEPSPs in either in wild-type or ST8Sia-II deficient samples.

[0046] A single train of high-frequency stimulation (1xHFS, applied in the presence of AP-5) induced robust PTP and LTP in slices from wild-type mice ($1133.1 \pm 180.4\%$ and $195.8 \pm 33.3\%$, respectively; $n=6$, $N=5$). The levels of PTP and LTP in ST8Sia-II deficient mice were $912.3 \pm 135.8\%$ and $181.6 \pm 13.1\%$, respectively ($n=5$, $N=3$) (Fig. 6b). This was not significantly different from values among wild-type littermates. Recorded profiles of CA3 LTP resembled those observed in our previous studies (Eckhardt et al., 2000; Evers et al., 2002) and by other groups (Maccaferri et al., 1998; Yeckel et al., 1999). PTP induced by a stronger induction protocol (4-HFS) was $1239.0 \pm 84.3\%$ ($n=7$, $N=5$) in wild-type and $1333.5 \pm 192.5\%$ ($n=6$, $N=4$) in ST8Sia-II deficient mice. The values measured 50-60 minutes after induction of LTP in wild-type and ST8Sia-II deficient mice were $219.2 \pm 24.1\%$ ($n=7$, $N=5$) and $257.2 \pm 32.7\%$ ($n=6$, $N=4$), respectively (data not shown). Thus, NMDA receptorindependent LTP in mossy fiber - CA3 synapses is not affected by ST8Sia-II deficiency.

Reduced fear conditioning responses and increased exploratory behavior

[0047] We examined ST8Sia-II deficient mice for physical, metabolic, and behavioral abnormalities, including assays of locomotor activity, muscle strength, heart rate, blood pressure, pulmonary function, nociception, and other parameters as presented in Table 1. There were no statistically significant differences between wild-type and ST8Sia-II deficient mice in these parameters. There were however consistent differences in exploratory activity, passive avoidance, and fear conditioning tasks that were replicated in two separate cohorts of mice.

[0048] The open field test measures exploration and anxiety behaviors in a novel environment. Mice are typically anxious in this context and tend to avoid the center of a large arena. The distance traveled in the center of the arena normalized for the total distance traveled is a measure of anxiety. ST8Sia-II deficient mice traveled more total distance in the open field ($t_{[48]} = 2.65$, $p < .01$) and more distance in the center of the arena ($t_{[48]} = 2.9$, $p < .005$) (Fig. 7a). Normalizing the distance traveled in the center to the total distance traveled revealed a trend ($p < .08$) of increased proportional time in the center, suggesting that ST8Sia-II deficient mice do not avoid the normally less preferred center area of the open field arena. In addition, increased rearing behavior, another indicator of exploratory activity, was observed among the second cohort of ST8Sia-II deficient mice tested with the mean

number of upper level photo-beams broken measured at 188 ± 16 for wild-type mice and 313 ± 42 for the ST8Sia-II deficient littermates ($t_{(1,19)} = 3.0$, $p < .01$).

[0049] In the passive avoidance task, the ST8Sia-II deficient mice were significantly impaired ($t_{(47)} = 2.79$, $p < .007$), failing to increase their latency to enter the dark chamber on the second day (Fig. 7b). There was no difference in latency to enter the dark chamber on the training day (wild-type: 40 ± 14 ; Δ/Δ : 36 ± 9).

[0050] Behavioral responses to two standard fear-conditioning tasks were also abnormal in ST8Sia-II deficient mice. The association of a single cue (i.e. a tone) with an unpleasant electrical shock is considered unimodal and critically depends upon neural processing in the amygdala but not hippocampus. In contrast, associating context (the spatial and environmental cues making up the test chamber) with the unpleasant stimulus is considered multimodal and requires neural processing in both amygdala and hippocampus (Fanselow and Le Doux, 1999). ST8Sia-II deficient mice were significantly impaired in both the cued ($t_{(48)} = 2.56$, $p < .01$) and contextual ($t_{(48)} = 2.23$, $p < .05$) versions of the fear conditioning test (Fig. 7b). ST8Sia-II deficient mice had a normal nociception response (Table 1) and were not impaired in the acoustic startle test (Fig. 7c), indicating that the deficit in fear conditioning to cue was not due to an inability to experience discomfort or to hear the tone.

[0051] ST8Sia-II deficient mice were also analyzed for spatial learning in the water maze test. NCAM-deficient mice exhibited a defect in this task, consistent with the finding of a defect in LTP in synapses formed by the Schaffer collaterals in the hippocampal CA1 region (Cremer et al., 1994; Muller et al., 1996). There was however no significant difference between the ST8Sia-II deficient and wild-type mice in the water maze acquisition trials or in probe trial performance (Fig. 7d), suggesting that spatial learning and associated memory are not altered by ST8Sia-II deficiency. This is also in accordance with the results of the electrophysiological measurements that showed normal LTP of hippocampal CA1 (and CA3) in the ST8Sia-II -deficient mice.

[0052] Performance of passive avoidance and fear conditioning tasks requires that the animals are able to control their movement. It was possible that if ST8Sia-II deficient mice were inherently hyperactive, and thereby would perform poorly without bearing impairments specifically in fear memory. For this reason, we quantitatively analyzed motor activity and basic physiologic

parameters over multiple light and dark cycles using automated metabolic chambers. It is noteworthy that ST8Sia-II deficient mice did not show an increase in motor activity and other parameters assessed, and continued to exhibit circadian rhythm (Fig. 7e). These results support the view that altered fear conditioning and exploratory behavior occurring in ST8Sia-II deficiency are due to alterations in processing and accessing the stimuli leading to provoking anxiety and fear memory.

[0053] It is widely accepted that the amygdala is involved in fear memory (LeDoux, 2000; Maren, 2001). Since PSA is expressed in the amygdala (Nacher, 2002), we investigated possible PSA alterations in ST8Sia-II deficiency. We detected similar PSA expression in the amygdala, hypothalamus, and piriform cortex of adult ST8Sia-II deficient mice and wildtype littermates (data not shown), indicating that PSA deficiency does not occur in this ST8Sia-II deficient model of defective fear conditioning. Furthermore, retrograde labeling with BDA injected into the amygdala demonstrated a normal trace pattern in the hippocampus of ST8Sia-II deficient mice (data not shown), as compared with previous findings (Pikkarainen et al., 1999; Berretta et al., 2001; Petrovich et al., 2001).

Differential expression and activity of ST8Sia-II and ST8Sia-IV polysialyltransferases

[0054] The ST8Sia-II polysialyltransferase is required for the formation of a subset of the total PSA biosynthetic repertoire expressed in the brain. We further observed that ST8Sia-II forms PSA in a spatial and temporal pattern that functions distinctly from PSA produced by ST8Sia-IV. We also noted partial overlap with the NCAM deficient phenotype, suggesting that the functions of NCAM are in some contexts dependent upon PSA modification by ST8Sia-II. Deficiency of ST8Sia-II caused an abnormality in the targeting of infrapyramidal hippocampal mossy fibers resulting in ectopic synapse formation in CA3.

[0055] Neural cell adhesion, migration, axonal growth and neuronal plasticity have been clearly attributed to PSA, although the relative contribution of ST8Sia-II, ST8Sia-IV, and NCAM to these events is not completely defined. During development, ST8Sia-II contributes to the majority of PSA formation in specific brain regions, including granule cells of the dentate gyrus and neural precursor cells in the SVZ. However, PSA deficiency by ST8Sia-II inactivation does not alter mitotic events in neurogenesis. In neuronal differentiation, PSA remains expressed on mossy fiber

axons and migrating cells in the RMS or striatum, most likely due to the activity of ST8Sia-IV. In fact, adult mice lacking ST8Sia-IV are highly deficient in PSA among multiple brain compartments including the mossy fibers and striatum (Eckhardt et al., 2000). These results indicate different contributions by ST8Sia-II and ST8Sia-IV to PSA formation involving temporal and likely cell-type-specificities that promote the unique functions that can now be ascribed to these two polysialyltransferases.

[0056] Migrating cells in the RMS express PSA in the absence of either ST8Sia-II or ST8Sia-IV suggesting that in some contexts the functions of both polysialyltransferases may also overlap. Tangential migration from the SVZ to the olfactory bulb is a relatively long distance, and both polysialyltransferases may operate in this migration. In contrast, even though granule cells express both ST8Sia-II and ST8Sia-IV transcripts (Angata et al., 1997; Hildebrandt et al., 1998), they appear to express PSA initially by ST8Sia-II, but subsequently by ST8Sia-IV when they extend mossy fiber axons. It is therefore also possible that PSA synthesis may be further regulated at the level of polysialyltransferase RNA translation.

Distinct and overlapping functions of polysialyltransferases and NCAM

[0057] From characterization of mice deficient in NCAM, ST8Sia-II, or ST8Sia-IV, we can compare the biological roles of PSA and NCAM (Table 2). NCAM-deficient mice (intact ST8Sia-II and ST8Sia-IV expression), and mice treated with endo-N to remove PSA, have a thicker RMS and a smaller olfactory bulb, perhaps due to slower tangential migration of precursor cells (Hu et al., 1996). In contrast, mice lacking either ST8Sia-II or ST8Sia-IV have a normal RMS and olfactory bulb, suggesting that PSA produced by either ST8Sia-II or ST8Sia-IV is sufficient for olfactory precursor cells to migrate properly, or that additional polysialyltransferases operate in the synthesis of PSA in these cells.

[0058] All studied forms of short- and long-term hippocampal synaptic plasticity appeared to be normal in adult ST8Sia-II deficient mice. In contrast, adult ST8Sia IV-deficient mice are deficient in LTP and LTD in the hippocampal CA1 region (Eckhardt et al., 2000). This is consistent with low levels of ST8Sia-II expression in adulthood and the continued expression of ST8Sia-IV in the hippocampus of adult ST8Sia-II deficient mice. These studies underscore the unique role of ST8Sia-IV in the formation of CA1 LTP in adult mice. NMDA receptor-independent LTP in

hippocampal CA3 pyramidal cells was abolished in NCAM-deficient mice (Cremer et al., 1998). This contrasts with findings of normal CA3 LTP in adult mice lacking either ST8Sia-II or ST8Sia-IV, or ST8Sia-IV deficient mice treated with endo-N (Eckhardt et al., 2000). Taken together these findings support the view that the NCAM protein backbone is required for LTP in the CA3 region of the adult hippocampus.

Polysialic acid in axon targeting and synapse formation

[0059] When axons are misguided and do not meet the proper target cells, they are typically retracted and eventually die (Tessier-Lavigne and Goodman, 1996; Pettmann and Henderson, 1998; Dickson, 2002). The hippocampal mossy fiber pathway from the granule cells of the dentate gyrus to the pyramidal cells of CA3 is a particularly interesting system for studying these processes. Neural precursor cells arise in the most inner layer of the dentate gyrus, and subsequently migrate into the granule cell layer, where they differentiate into granular neurons that extend dendrites and axons (Seki and Arai, 1993; Gage, 2000). The suprapyramidal bundle of mossy fiber axons, which also express PSA, target towards CA3 pyramidal cells to form synapses. The infrapyramidal mossy fibers, the secondary blade of mossy fiber axons, initially project into the area below CA3 pyramidal cells and merge with suprapyramidal mossy fibers after crossing through the pyramidal cell layer (Gaarskjaer, 1986).

[0060] We observed abnormal axonal targeting of the infrapyramidal mossy fiber projection in ST8Sia-II deficient mice, and although these axons continued to express PSA, they formed ectopic synapses in the CA3a region. NCAM180-deficient mice exhibit a similar altered morphology of infrapyramidal mossy fiber projection (Seki and Rutishauser, 1998). In contrast, this phenotype was not observed among ST8Sia-IV deficient mice, indicating that correct targeting of infrapyramidal mossy fiber projections involves a function of PSA that is dependent upon ST8Sia-II and NCAM (Table 2).

ST8Sia-II and PSA in fear and anxiety behaviors

[0061] Infrapyramidal mossy fiber projections vary among different mouse and rat strains and appear to correlate with reduced anxiety, increased exploration, and reduced responses to fear conditioning (van Daal et al., 1991; Henze et al., 2000). In the open field test, inbred mouse strains

with larger intra- and infrapyramidal mossy fiber fascicles habituate faster to a novel environment and have reduced fear behavior (Crusio, 2001). Additionally, mice engineered with a defective *Dcx* gene, a cause of classical type 1 lissencephaly in human, have a similar defect in mossy fiber projection and exhibit reduced freezing to conditioned fear assays in both cue- and context-associated tasks (Corbo et al., 2002). In rats, the DA rat strain exhibits significantly larger infrapyramidal mossy fibers with reduced freezing and high rearing activities, whereas BDE rats with shorter infrapyramidal mossy fibers show freezing and low rearing activity (Prior et al., 1997). These behavioral changes are similar in CHL1 mutant mice that also have larger intra- and infrapyramidal mossy fiber projections (Montag-Sallaz et al., 2002).

[0062] ST8Sia-II deficiency alters fear responses normally processed by both the hippocampus and amygdala. Although ST8Sia-IV deficient mice have not been similarly studied, NCAM deficiency leads to the behavioral changes detected in ST8Sia-II deficiency (Stork et al., 2000). In contrast to ST8Sia-II deficiency, NCAM deficiency also resulted in impaired spatial learning memory, which is consistent with the impairment of LTP in Schaffer collaterals of the CA1 region (Cremer et al., 1994; Muller et al., 1996).

[0063] Genetic control of ST8Sia-II and ST8Sia-IV expression appears to underlie the distinct neurological processes mediated by PSA function. PSA can play different roles in axonal projections that may also reflect the strength of axon-axon and axon-environment interactions (Marx et al., 2001). In the adult hippocampus, chronic stress as well as treatment with glucocorticoid stress hormones alters neural plasticity involving mossy fiber terminals and CA3 pyramidal cells, which may reflect the associated changes in hippocampal PSA and NCAM expression (Rodriguez et al., 1998; Sandi et al., 2001; 2003). Furthermore, kindling of the amygdala, but not the entorhinal cortex, induces sprouting of infrapyramidal mossy fibers in the CA3 region (Reprea et al., 1989).

References

Ammassari-Teule M, Pavone F, Castellano C, McGaugh JL (1991) Amygdala and dorsal hippocampus lesions block the effects of GABAergic drugs on memory storage. *Brain Res.* 551:104-109.

Anagnostaras SG, Gale GD, Fanselow MS (2001) Hippocampus and contextual fear conditioning: recent controversies and advances. *Hippocampus* 11:8-17.

Angata K, Nakayama J, Fredette B, Chong K, Ranscht B., Fukuda M (1997) Human STX polysialyltransferase forms the embryonic form of the neural cell adhesion molecule. Tissue specific expression, neurite outgrowth, and chromosomal localization in comparison with another polysialyltransferase, PST. *J. Biol. Chem.* 272:7182-7190.

Angata K, Fukuda M. (2003) Polysialyltransferases: major players in polysialic acid synthesis on the neural cell adhesion molecule. *Biochimie* 85:195-206.

Bagri A, Cheng H, Yaron A, Pleasure SJ, Tessier-Lavigne M (2003) Stereotyped pruning of long hippocampal axon branches triggered by retraction inducers of the semaphorin family. *Cell* 113:285-299.

Becker CG, Artola A, Gerardy-Schahn R, Becker T, Welzl H, Schachner M (1996) The polysialic acid modification of the neural cell adhesion molecule is involved in spatial learning and hippocampal long-term potentiation. *J. Neurosci. Res.* 45:143-152.

Berretta S, Munno DW, Benes FM (2001) Amygdala activation alters the hippocampal GABA system: "partial" modelling for postmortem changes in schizophrenia. *J. Comp. Neurol.* 431:129-138.

Bruses JL, Rutishauser U (2001) Roles, regulation, and mechanism of polysialic acid function during neural development. *Biochimie* 83:635-643.

Cheng H, Bagri A, Yaron A, Stein E, Pleasure SJ, Tessier-Lavigne M (2001) Plexin-Ameliorating mediates semaphorin signaling and regulates the development of hippocampal axonal projections. *Neuron* 32:249-263.

Claiborne BJ, Xiang Z, Brown TH (1993). Hippocampal circuitry complicates analysis of long-term potentiation in mossy fiber synapses. *Hippocampus* 3:115-121.

Corbo JC, Deuel TA, Long JM, LaPorte P, Tsai E, Wynshaw-Boris A, Walsh CA (2002). Doublecortin is required in mice for lamination of the hippocampus but not the neocortex. *J. Neurosci.* 22:7548-7557.

Cremer H, Lange R, Christoph A, Plomann M, Vopper G, Roes J, Brown R, Baldwin S, Kraemer P, Scheff S, Barthels D, Rajewsky K, Wille W (1994) Inactivation of the N-CAM gene in mice results in size reduction of the olfactory bulb and deficits in spatial learning. *Nature* 367:455-459.

Cremer H, Chazal G, Goridis C, Represa A (1997) NCAM is essential for axonal growth and fasciculation in the hippocampus. *Mol. Cell. Neurosci.* 8:323-335.

- Cremer H, Chazal G, Carleton A, Goridis C, Vincent JD, Lledo PM (1998) Long-term but not short-term plasticity at mossy fiber synapses is impaired in neural cell adhesion molecule-deficient mice. *Proc. Natl. Acad. Sci. USA* 95:13242-13247.
- Cremer H, Chazal G, Lledo PM, Rougon G, Montaron MF, Mayo W, Le Moal M, Abrous DN (2000) PSA-NCAM: an important regulator of hippocampal plasticity. *Int. J. Dev. Neurosci.* 18:213-220.
- Crusio WE (2001) Genetic dissection of mouse exploratory behaviour. *Behav. Brain Res.* 125:127-132.
- Datta AK, Paulson JC (1995) The sialyltransferase "sialylmotif" participates in binding the donor substrate CMP-NeuAc. *J. Biol. Chem.* 270:1497-1500.
- Dickson BJ (2002) Molecular mechanisms of axon guidance. *Science* 298:1959-1964.
- Eckhardt M, Mühlenhoff M, Bethe A, Koopman J, Frosch M, Gerardy-Schahn R. (1995) Molecular characterization of eukaryotic polysialyltransferase-I. *Nature* 373:715-718.
- Eckhardt M, Gerardy-Schahn R. (1998) Genomic organization of the murine polysialyltransferase gene ST8SiaIV (PST-1). *Glycobiology* 8:1165-1172.
- Eckhardt M, Bukalo O, Chazal G, Wang L, Goridis C, Schachner M, Gerardy-Schahn R, Cremer H, Dityatev A (2000) Mice deficient in the polysialyltransferase ST8SiaIV/PST-1 allow discrimination of the roles of neural cell adhesion molecule protein and polysialic acid in neural development and synaptic plasticity. *J. Neurosci.* 20:5234-5244.
- Edwards FA, Konnerth A, Sakmann B (1990) Quantal analysis of inhibitory synaptic transmission in the dentate gyrus of rat hippocampal slices: a patch-clamp study. *J. Physiol.* 430:213-249.
- Evers MR, Salmen B, Bukalo O, Rollenhagen A, Bosl MR, Morellini F, Bartsch U, Dityatev A, Schachner M (2002) Impairment of L-type Ca^{2+} channel-dependent forms of hippocampal synaptic plasticity in mice deficient in the extracellular matrix glycoprotein tenascin-C. *J. Neurosci.* 22:7177-7194.
- Fanselow MS, LeDoux JE (1999) Why we think plasticity underlying Pavlovian fear conditioning occurs in the basolateral amygdala. *Neuron* 23:229-232.
- Franklin KBJ, Paxinos G (1996) The mouse brain in stereotaxic coordinates. (San Diego: Academic Press).
- Fujimoto I, Bruses JL, Rutishauser U (2001) Regulation of cell adhesion by polysialic acid. Effects on cadherin, immunoglobulin cell adhesion molecule, and integrin function and independence from neural cell adhesion molecule binding or signaling activity. *J. Biol. Chem.* 276:31745-31751.

- Gaarskjaer FB (1986) The organization and development of the hippocampal mossy fiber system. *Brain Res.* 396:335-357.
- Gage FH (2000) Mammalian neural stem cells. *Science* 287:1433-1438.
- Hallenbeck PC, Vimr ER, Yu F, Bassler B, Troy FA (1987) Purification and properties of a bacteriophage-induced endo-N-acetylneuraminidase specific for poly-alpha-2,8-sialosyl carbohydrate units. *J. Biol. Chem.* 262:3553-3561.
- Henze DA, Urban NN, Barrionuevo G (2000) The multifarious hippocampal mossy fiber pathway: a review. *Neuroscience* 98:407-427.
- Hildebrandt H, Becker C, Murau M, Gerardy-Schahn R, Rahmann H (1998) Heterogeneous expression of the polysialyltransferases ST8Sia-II and ST8Sia IV during postnatal rat brain development. *J. Neurochem.* 71:2339-2348.
- Hu H, Tomasiewicz H, Magnuson T, Rutishauser U (1996) The role of polysialic acid in migration of olfactory bulb interneuron precursors in the subventricular zone. *Neuron* 16:735-743.
- Kiss JZ, Troncoso E, Djebbara Z, Vutsits L, Muller D (2001) The role of neural cell adhesion molecules in plasticity and repair. *Brain Res. Brain Res. Rev.* 36:175-184.
- Kojima N, Yoshida Y, Tsuji S (1995) A developmentally regulated member of the sialyltransferase family (ST8Sia-II, STX) is a polysialic acid synthase. *FEBS Lett.* 373:119-122.
- Kuhn HG, Dickinson-Anson H, Gage FH (1996) Neurogenesis in the dentate gyrus of the adult rat: age-related decrease of neuronal progenitor proliferation. *J. Neurosci.* 16:2027-2033.
- Kurosawa N, Yoshida Y, Kojima N, Tsuji S (1997) Polysialic acid synthase (ST8Sia-II /STX) mRNA expression in the developing mouse central nervous system. *J. Neurochem.* 69:494-503.
- LeDoux JE (2000) Emotion circuits in the brain. *Annu. Rev. Neurosci.* 23:155-184.
- Lisman JE (1999) Relating hippocampal circuitry to function: recall of memory sequences by reciprocal dentate-CA3 interactions. *Neuron* 22:233-242.
- Maccaferri G, Toth K, McBain CJ (1998) Target-specific expression of presynaptic mossy fiber plasticity. *Science* 279:1368-1370.
- Maren S (2001) Neurobiology of Pavlovian fear conditioning. *Annu. Rev. Neurosci.* 24:897-931.
- Marth JD (1996) Recent advances in gene mutagenesis by site-directed recombination. *J. Clin. Invest.* 97:1999-2002.
- Marx M, Rutishauser U, Bastmeyer M (2001) Dual function of polysialic acid during zebrafish central nervous system development. *Development* 128:4949-4958.

McIlwain KL, Merriweather MY, Yuva-Paylor LA, Paylor R. (2001) The use of behavioral test batteries: effects of training history. *Physiol. Behav.* 73:705-717.

Montag-Sallaz M, Schachner M, Montag D (2002) Misguided axonal projections, neural cell adhesion molecule 180 mRNA upregulation, and altered behavior in mice deficient for the close homolog of L1. *Mol. Cell. Biol.* 22:7967-7981.

Muller D, Wang C, Skibo G, Toni N, Cremer H, Calaora V, Rougon G, Kiss JZ (1996) PSA-NCAM is required for activity-induced synaptic plasticity. *Neuron* 17:413-422.

Nacher J, Lanuza E, McEwen BS (2002) Distribution of PSA-NCAM expression in the amygdala of the adult rat. *Neuroscience* 113:479-484.

Nakayama J, Fukuda MN, Fredette B, Ranscht B, Fukuda M (1995) Expression cloning of a human polysialyltransferase that forms the polysialylated neural cell adhesion molecule present in embryonic brain. *Proc. Natl. Acad. Sci. USA* 92:7031-7035.

Ong E, Nakayama J, Angata K, Reyes L, Katsuyama T, Arai Y, Fukuda M (1998) Developmental regulation of polysialic acid synthesis in mouse directed by two polysialyltransferases, PST and STX. *Glycobiology* 8:415-424.

Pasterkamp RJ, Kolodkin AL (2003) Semaphorin junction: making tracks toward neural connectivity. *Curr. Opin. Neurobiol.* 13:79-89.

Petrovich GD, Canteras NS, Swanson LW (2001) Combinatorial amygdalar inputs to hippocampal domains and hypothalamic behavior systems. *Brain Res. Brain Res. Rev.* 38:247-289.

Pettmann B, Henderson CE (1998) Neuronal cell death. *Neuron* 20:633-647.

Pikkarainen M, Ronkko S, Savander V, Insausti R, Pitkanen A (1999) Projections from the lateral, basal, and accessory basal nuclei of the amygdala to the hippocampal formation in rat. *J. Comp. Neurol.* 403:229-260.

Prior H, Schwegler H, Ducker G (1997) Dissociation of spatial reference memory, spatial working memory, and hippocampal mossy fiber distribution in two rat strains differing in emotionality. *Behav. Brain Res.* 87:183-194.

Rodriguez JJ, Montaron MF, Petry KG, Aourousseau C, Marinelli M, Premier S, Rougon G, Le Moal M, Abrous DN (1998) Complex regulation of the expression of the polysialylated form of the neuronal cell adhesion molecule by glucocorticoids in the rat hippocampus. *Eur. J. Neurosci.* 10:2994-3006.

Rutishauser U, Landmesser L (1996) Polysialic acid in the vertebrate nervous system: a promoter of plasticity in cell-cell interactions. *Trends Neurosci.* 19:422-427.

Rutishauser U (1998) Polysialic acid at the cell surface: biophysics in service of cell interactions and tissue plasticity. *J. Cell Biochem.* 70:304-312.

Sandi C, Merino JJ, Cordero MI, Touyarot K, Venero C (2001) *Neuroscience* 102:329-339.

Sandi C, Merino JJ, Cordero MI, Kruyt ND, Murphy KJ, Regan CM (2003) *Biol. Psychiatry* 54:599-607.

Schachner M, Martini R (1995) Glycans and the modulation of neural-recognition molecule function. *Trends Neurosci.* 18:183-191.

Scheidegger EP, Sternberg LR, Roth J, Lowe JB (1995) A human STX cDNA confers polysialic acid expression in mammalian cells. *J. Biol. Chem.* 270:22685-22688.

Seki T, Arai Y (1993) Distribution and possible roles of the highly polysialylated neural cell adhesion molecule (NCAM-H) in the developing and adult central nervous system. *Neurosci. Res.* 17:265-290.

Seki T, Rutishauser U (1998) *J. Neurosci.* 18:3757-3766.

Skutella T, Nitsch R (2001) *Trends Neurosci.* 24:107-113.

Stork O, Welzl H, Wolfer D, Schuster T, Mantei N, Stork S, Hoyer D, Lipp H, Obata K, Schachner M. (2000) *Eur. J. Neurosci.* 12:3291-3306.

Takashima S, Yoshida Y, Kanematsu T, Kojima N, Tsuji S (1998) *J. Biol. Chem.* 273:7675-7683.

Tessier-Lavigne M, Goodman CS (1996) *Science* 274:1123-1133.

Tomasiewicz H, Ono K, Yee D, Thompson C, Goridis C, Rutishauser U, Magnuson T (1993) *Neuron* 11:1163-1174.

van Daal JHHM, Herbergs PJ, Crusio WE, Schwegler H, Jenks BG, Lemmens WAJG, van Abeelen JHF (1991) *Behav. Brain Res.* 43:57-64.

Weisskopf MG, Castillo PE, Zalutsky RA, Nicoll RA (1994) *Science* 265:1878-1882.

Yeckel MF, Kapur A, Johnston D (1999) *Nat. Neurosci.* 2:625-633.

Yoshida Y, Kurosawa N, Kanematsu T, Kojima N, Tsuji S (1996) *J. Biol. Chem.* 271:30167-30173.

Table 1. Assessments of basic appearance, function and metabolic parameters.

Test / Assay	wt/wt Mean (SEM)	Δ/Δ Mean (SEM)
Gross Physical Assessment:		
General appearance	Normal	Normal
Sensorimotor reflexes	Normal	Normal
Postural reflexes	Normal	Normal
Motor activity:		
Rotarod (latency to fall-sec)	35.7 (10.4)	27.5 (2.6)
Initiation of movement (sec)	13.2 (3.8)	16.2 (3.1)
Wire hang (latency to fall-sec)	28.6 (4.5)	30.1 (3.1)
Grip strength (force in grams)	373.8 (65.6)	393.2 (71.8)
Cage-top hang test (latency to fall- sec)	38.4 (7.1)	23.6 (7.3)
Pole test (score)	5.3 (0.6)	5.1 (0.6)
Nociception:		
Hot plate (sec)	10.6 (1.2)	12.1 (1.9)
Tail flick (sec)	3.0 (0.17)	3.5 (0.52)
Blood pressure:		
Mean (dbp + 1/3(spb-dbp))	95.7 (4.4)	90.0 (5.2)
Systolic (sbp)	144.6 (6.5)	140.3 (9.2)
Diastolic (dbp)	72.3 (4.8)	67.3 (4.1)
Heart rate (bpm)	680 (10.9)	655 (14.3)
Pulmonary function - CO uptake (microliter/min)	27.9 (1.2)	25.5 (1.3)
Respiration rate (bpm)	239 (11.4)	231 (11.0)

Table 2. Comparison of polysialic acid and NCAM function in neural development and synaptic plasticity

Function	Endo-N	ST8Sia-IV deficiency	NCAM deficiency	ST8Sia-II deficiency	Basis of Defect
Migration of neural precursors	-	+	-	+	PSA-dependent NCAM function
LTP in CA1	-	- ^b	-	+	PSA- and ST8Sia-IV-dependent NCAM function
LTP in CA3	+ ^a	+	-	+	PSA-independent NCAM function
Lamination of mossy fibers	-	+	-	-	PSA- and ST8Sia-II-dependent NCAM function

Comparison includes present study and is revised from Eckhardt *et al.*, *J. Neurosci.*, 2000, 20: 5234-5244.

-, Impairment of function; +, normal function

^a In ST8Sia-IV deficient mice

^b Only in adult mice

Abstract

The invention provides methods and compositions for treating anxiety and fear disorders through inhibition of sialyl transferase activity.

This Page Is Inserted by IFW Operations
and is not a part of the Official Record

BEST AVAILABLE IMAGES

Defective images within this document are accurate representations of the original documents submitted by the applicant.

Defects in the images may include (but are not limited to):

- BLACK BORDERS
- TEXT CUT OFF AT TOP, BOTTOM OR SIDES
- FADED TEXT
- ILLEGIBLE TEXT
- SKEWED/SLANTED IMAGES
- COLORED PHOTOS
- BLACK OR VERY BLACK AND WHITE DARK PHOTOS
- GRAY SCALE DOCUMENTS

IMAGES ARE BEST AVAILABLE COPY.

**As rescanning documents *will not* correct images,
please do not report the images to the
Image Problem Mailbox.**

Fig. 1

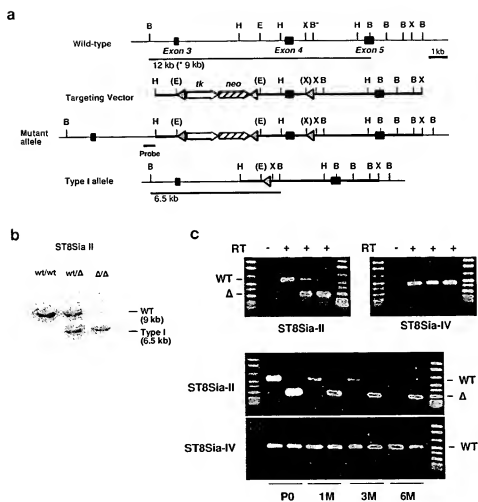


Fig. 2

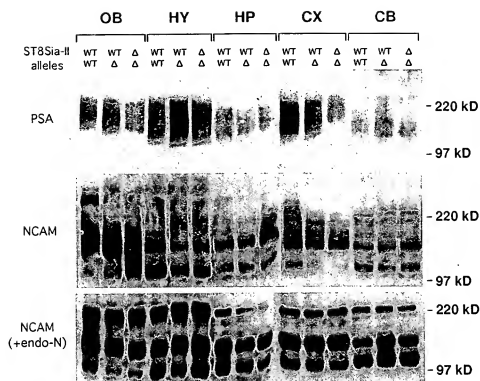


FIGURE 3

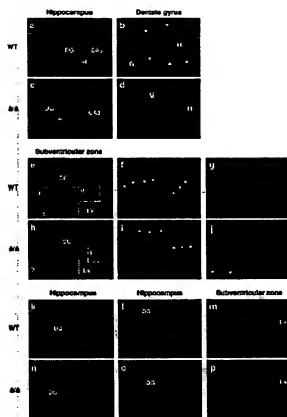


FIGURE 4

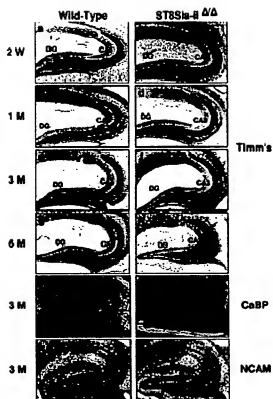


FIGURE 5

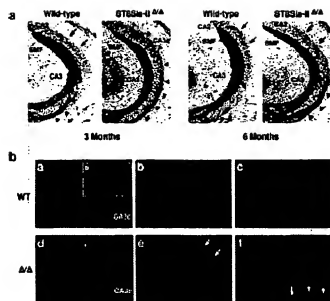


FIGURE 6

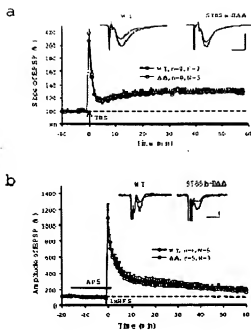
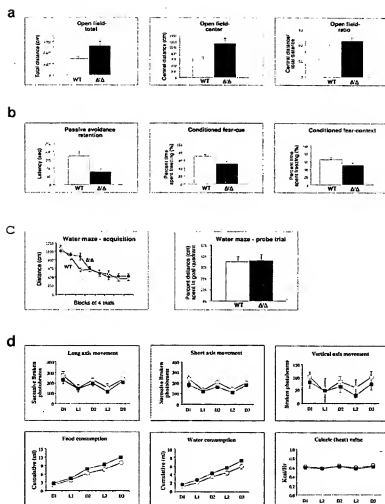


Fig. 7



Application Data Sheet

Application Information

Application Type::	Provisional
Subject Matter::	Utility
Suggested Group Art Unit::	N/A
CD-ROM or CD-R?::	None
Sequence submission?::	None
Computer Readable Form (CRF)?::	No
Title::	ANXIOLYTIC TREATMENT BY INHIBITION OF ST8SIA-II SIALYLTRANSFERASE
Attorney Docket Number::	220003065000
Request for Early Publication?::	No
Request for Non-Publication?::	No
Total Drawing Sheets::	7
Small Entity?::	Yes
Petition included?::	No
Secrecy Order in Parent Appl.?::	No

Applicant Information

Applicant Authority Type::	Inventor
Status::	Full Capacity
Given Name::	Jamey
Middle Name::	D.
Family Name::	MARTH
City of Residence::	San Diego
State or Province of Residence::	CA
Country of Residence::	US
Street of mailing address::	6247 Canyon Bluff Court
City of mailing address::	San Diego
State or Province of mailing address::	CA
Postal or Zip Code of mailing address::	92121

Applicant Authority Type::	Inventor
Status::	Full Capacity
Given Name::	Minoru
Family Name::	FUKUDA
City of Residence::	La Jolla
State or Province of Residence::	CA
Country of Residence::	US
Street of mailing address::	The Burnham Institute
City of mailing address::	La Jolla
State or Province of mailing address::	CA

Correspondence Information

Correspondence Customer Number::	25225
----------------------------------	-------

Representative Information

Representative Customer Number::	25225
----------------------------------	-------